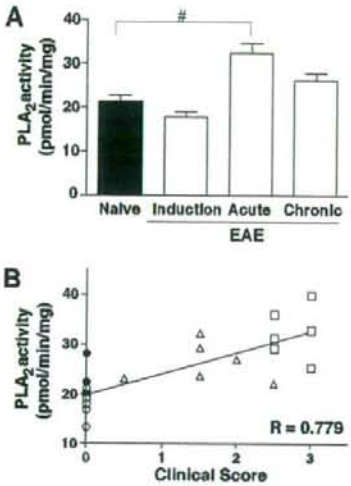

FIGURE 4. PLA_2 activity in SCs of naive and EAE mice. *A*, PLA_2 activity in SCs of naive mice and EAE mice in the induction, acute, and chronic phases ($n = 6$ animals) was measured using mixed micelles containing 1-palmitoyl-2-[^{14}C]arachidonoyl-PC and Triton X-100 in the presence of Ca^{2+} and DTT. Data represent means ± SEM. #, $p < 0.001$ by ANOVA with the Tukey-Kramer test. *B*, PLA_2 activity in naive (●) and EAE mice in the induction (○), acute (□), and chronic (△) phases is positively correlated with the clinical score ($p < 0.0001$ by the Spearman rank correlation test). Each data point represents the result from a single animal.

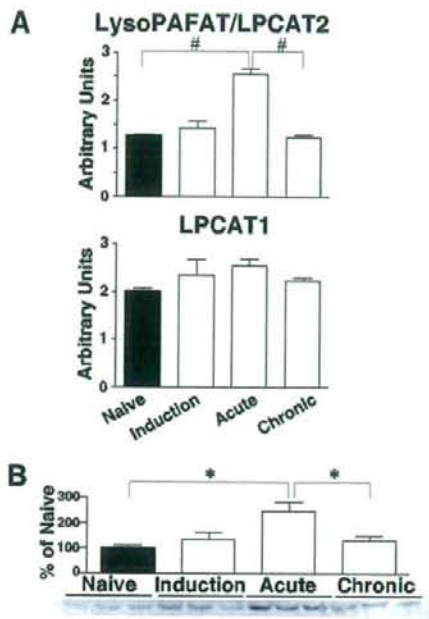

FIGURE 5. LysoPAFAT/LPCAT2 expression in SCs of naive and EAE mice. Expression levels of LysoPAFAT/LPCAT2 and LPCAT1 mRNAs (*A*) and LysoPAFAT/LPCAT2 proteins (*B*) were quantified by real-time PCR and Western blotting with densitometry, respectively, in SCs of naive mice and EAE mice in the induction, acute, and chronic phases ($n = 6$ animals). A representative blot from two independent experiments is shown for LysoPAFAT ($n = 3$ animals). Data represent means ± SEM. #, $p < 0.001$ and *, $p < 0.05$ by ANOVA with the Tukey-Kramer test.

Western blotting

Ten micrograms of protein was resolved by 10% SDS-PAGE and transferred to a Hybond ECL nitrocellulose membrane (GE Healthcare Bio-Sciences). The membrane was blocked with 5% skim milk and incubated with anti-LysoPAFAT antiserum (Immuno-Biological Laboratories). After washing, the membranes were incubated with HRP-linked anti-rabbit IgG (GE Healthcare BioSciences), washed, and then exposed to the Western blotting detection reagents (GE Healthcare BioSciences). The membranes were scanned with a LAS-4000 luminescent image analyzer (Fuji film).

Primary culture

Primary young cortical neurons were prepared from C57BL/6 mouse brains on embryonic day 13 as previously described (28, 29). Primary astrocytes and microglia were obtained from cerebral hemispheres of C57BL/6 mouse brains on postnatal day 1, as previously described, with minor modifications (28–30). Briefly, after a 14-day culture period, astrocytes were purified by two passages. Microglia was prepared as a floating cell suspension and transferred to culture dishes. Unattached cells were removed before isolating total RNA. The purities of astrocytes and microglia were estimated to be >90% and >99%, respectively, by immunostaining for glial fibrillary acidic protein (GFAP) and Iba1. Total RNA (1 μg) was reverse-transcribed as described above.

$CD4^+$ and $CD8^+$ T cells were obtained from spleens of C57BL/6 mice using a MACS magnetic cell separation system (Miltenyi Biotec). The purities of $CD4^+$ and $CD8^+$ T cells were estimated to be >90% by flow cytometry (Beckman Coulter). T cells were stimulated with or without anti-CD3e Ab (BD Biosciences) for 24 h, followed by reverse transcription of total RNA (100 ng) as described above.

Statistical analysis

Results are expressed as means ± SEM. Data were analyzed statistically by means of ANOVA with the Tukey-Kramer post hoc test, the Kruskal-Wallis test with Dunn's post hoc test, or the Spearman rank correlation test as appropriate, using GraphPad PRISM software. Values of $p < 0.05$ were considered to be statistically significant. Cluster analysis was performed using JMP6 software (Hulinks).

Results

Elevation of PAF levels in SCs of EAE mice

C57BL/6 female mice were immunized with MOG_{35-55} and clinical symptoms were monitored (Fig. 2*A*). All mice developed EAE and the mean maximal clinical score was 2.6 ± 0.16 ($n = 8$ animals). To confirm our previous report, PAF levels in SCs were measured by HPLC-ESI-MS/MS. The SCs were collected from naive mice and immunized mice in the induction, acute, and chronic phases of EAE (Fig. 2*A*). PAF levels were significantly elevated in the acute phase (Fig. 2*B*) and positively correlated with the clinical score ($p < 0.0001$; Fig. 2*C*). Thus, the fluctuation in PAF levels during the disease course was reproduced (16). These results demonstrate that the metabolism of PAF (Fig. 1) in the SC was perturbed by the pathogenesis of EAE. Therefore, we determined the enzymes that synthesize and degrade PAF using EAE mice.

Up-regulation of PLA_2 mRNA expression and activity in SCs of EAE mice

The various PLA_2 (groups IVA, IVB, IVC, IVD, IVE, and IVF $cPLA_2$s, groups V and X $sPLA_2$s, and group VI $iPLA_2$) mRNA levels were determined by quantitative RT-PCR to elucidate the effects of PLA_2s on PAF production. Group IVA $cPLA_2$ and group V $sPLA_2$ mRNA levels were elevated in the acute phase of EAE and decreased in the chronic phase to a level that was still higher than that in naive mice (Fig. 3*A*). The relationships among the mRNA levels were evaluated by cluster analysis that distinguished group IVA $cPLA_2$ and group V $sPLA_2$ from other PLA_2s (Fig. 3*B*). In addition, the poorly characterized groups IVB and IVF

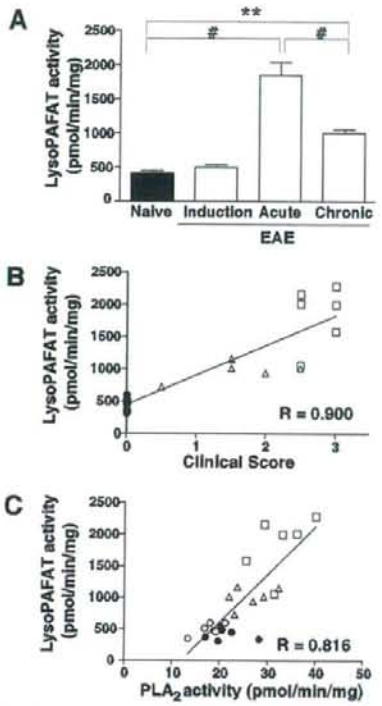

FIGURE 6. LysoPAFAT activity in SCs of naive and EAE mice. *A*, LysoPAFAT activity in SCs of naive mice and EAE mice in the induction, acute, and chronic phases ($n = 6$ animals) was measured as described in *Materials and Methods*. Data represent means ± SEM. #, $p < 0.001$ and **, $p < 0.01$ by ANOVA with the Tukey-Kramer test. *B* and *C*, LysoPAFAT activity in SCs of naive (●) and EAE mice in the induction (○), acute (□), and chronic (△) phases is positively correlated with the clinical score (*B*; $p < 0.0001$ by the Spearman rank correlation test) and PLA_2 activity (*C*; $p < 0.0001$). Each data point represents the results from a single animal.

cPLA$_2$s were up-regulated and clustered together (Fig. 3, *A* and *B*). PLA_2 activity was measured using 1-palmitoyl-2-[^{14}C]arachidonoyl-PC as a substrate with Ca^{2+} and DTT. The enzyme activity increased with the progression of EAE pathology ($p < 0.001$; Fig. 4*A*) and correlated significantly with the clinical score ($p < 0.0001$; Fig. 4B). These results suggest that PAF accumulation in SCs of EAE mice may be due to an up-regulation of PLA_2 and lysoPAFAT (see below).

Enhancement of LysoPAFAT/LPCAT2 expression and activity in SCs of EAE mice

To examine the involvement of LysoPAFAT/LPCAT2, expression levels of the transcripts and proteins were examined in SCs of naive and EAE mice by quantitative RT-PCR and Western blotting, respectively. LysoPAFAT/LPCAT2 transcripts and proteins were elevated in the acute phase and then declined in the chronic phase of EAE (Fig. 5). In contrast, mRNA expression level of the homologous enzyme LPCAT1 was unaltered during the disease course (Fig. 5). In agreement with these observations, the enzyme activities in the acute and chronic phases were higher than those of naive mice ($p < 0.001$; Fig. 6*A*). We found a significantly positive correlation between the clinical score and the LysoPAFAT activity ($p < 0.0001$; Fig. 6*B*). Furthermore, LysoPAFAT activity was

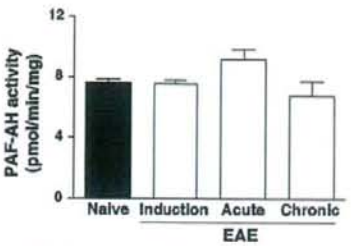

FIGURE 7. PAF-AH activity in SCs of naive and EAE mice. PAF-AH activity in SCs of naive mice and EAE mice in the induction, acute, and chronic phases ($n = 6$ animals) was measured as described in *Materials and Methods*. Data represent means ± SEM.

positively correlated with PLA_2 activity ($p < 0.001$; Fig. 6*C*). These results suggest that PAF accumulation in SCs of EAE mice is caused by the enhancement of LysoPAFAT/LPCAT2 expression and the corresponding increase in LysoPAFAT activity.

Unaltered basal PAF-AH activity in SCs of EAE mice

We investigated whether PAF-AH affected the accumulation of PAF in SCs of EAE mice. Although PAF-AH activity appeared to be slightly increased in the acute phase of EAE, the enzyme activity did not change significantly during the disease course (Fig. 7). PAF-AH activity did not correlate with the clinical score, PLA_2 activity, or LysoPAFAT activity (data not shown). Thus, PAF accumulation in SCs of EAE mice may be independent of the PAF degradation system.

LysoPAFAT/LPCAT2 expression in primary cultured murine microglia and astrocytes

We previously demonstrated LysoPAFAT/LPCAT2 mRNA expression in murine brain, macrophages, and neutrophils (12). Its expression was determined by RT-PCR and Western blotting in primary cultured murine neurons, astrocytes, microglia (Fig. 8), CD4$^+$ T cells, and CD8$^+$ T cells (data not shown). We found that LysoPAFAT/LPCAT2 mRNA was expressed in microglia and astrocytes, but not in neurons (Fig. 8*A*). The levels of LysoPAFAT/LPCAT2 transcripts were very low in both T cell subsets, with or without anti-CD3ε Ab stimulation for 24 h (data not shown). LysoPAFAT/LPCAT2 protein expression was observed in microglia, but not in astrocytes (Fig. 8*B*). These results suggest that PAF may

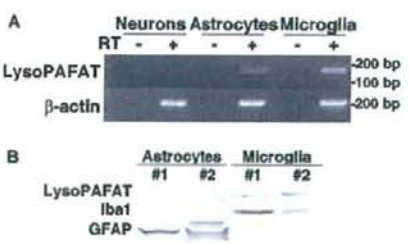

FIGURE 8. LysoPAFAT/LPCAT2 expression in the primary cultured cells of the murine CNS. *A*, LysoPAFAT/LPCAT2 and β-actin mRNA expression in primary cultured neurons, astrocytes, and microglia was determined by RT-PCR. The expected PCR products for LysoPAFAT and β-actin were 167 and 197 bp, respectively. *B*, Expression of LysoPAFAT/LPCAT2, Iba1, and GFAP in primary cultured astrocytes and microglia was determined by Western blotting. Each lane represents cells purified from an individual experiment.

be produced by activated microglia and infiltrating macrophages in SCs of EAE mice.

Discussion

In the present study, we have assessed the metabolic processing of PAF in SCs of naive and EAE mice to explain the enhanced PAF production in EAE mice. In general, accumulation of PAF can be accounted for by the up-regulation of the production system in the remodeling pathway and/or the down-regulation of the degradation system. We have demonstrated that the PAF production system is increased and the degradation system is unchanged in SCs during EAE.

The PAF production system in the remodeling pathway consists of two steps. The first step is production of the PAF precursor lyso-PAF by PLA_2s that hydrolyze the *sn*-2 acyl chain of PC (9) (Fig. 1). Several lines of evidence have suggested that group IVA $cPLA_2$, groups IIA and V $sPLA_2$s, and group VI $iPLA_2$ mRNAs are expressed in the SC of the naive rat (31, 32). In agreement with these studies, we have found that SCs of C57BL/6 mice express these PLA_2 mRNAs, with the exception of group IIA $sPLA_2$ (Fig. 3), which is absent in this mouse strain (33). Because the groups IVA, IVB, and IVF $cPLA_2$s and group V $sPLA_2$ mRNA levels are elevated in the acute phase of EAE (Fig. 3), lipid mediators produced by these four PLA_2s presumably participate in the pathogenesis of EAE. Although little is known about the functions of groups IVB and IVF $cPLA_2$s, it is generally accepted that group IVA $cPLA_2$ and group V $sPLA_2$ stimulate the arachidonic acid cascade (33). Indeed, hierarchical cluster analysis demonstrates the functional analogy of these PLA_2s in EAE pathology (Fig. 3*B*). EAE is not completely ameliorated in PAFR-KO mice (16), whereas group IVA $cPLA_2$ deficiency or treatments with PLA_2 inhibitors protect mice from the EAE pathology (17, 34). Eicosanoid levels were quantified simultaneously and we found that PGE_2 levels were dramatically changed during the disease course (Y. Kihara, S. Ishii, Y. Kita, S. Uematsu, S. Akira, and T. Shimizu, unpublished data). These data suggest that, not only PAF, but also eicosanoids downstream of PLA_2 are critical for the EAE pathology. We have demonstrated the elevation of PLA_2 activity in the acute phase of EAE using 1-palmitoyl-2-[^{14}C]arachidonoyl-PC as a substrate in the presence of Ca^{2+} and DTT (Fig. 4). Since this assay condition is optimized for group IV $cPLA_2$s (35), the elevated PLA_2 activity in the acute phase of EAE may be derived from groups IVA, IVB, and/or IVF $cPLA_2$s. However, groups IVB and IVF $cPLA_2$s have lower PLA_2 activity than group IVA $cPLA_2$ under the present assay conditions (24, 36, 37). Thus, group IVA $cPLA_2$ may be deeply involved in the up-regulation of PLA_2 activity in SCs of EAE mice. Additionally, group IVA $cPLA_2$ is essential for producing PAF, since PAF synthesis is significantly diminished in calcium ionophore-stimulated group IVA $cPLA_2$-deficient macrophages (11). These results suggest that the PAF precursor lyso-PAF is supplied primarily by group IVA $cPLA_2$ during EAE. Because Cunningham et al. (38) reported that $sPLA_2$ activity was up-regulated in urine of EAE rats and MS patients, it may play roles in the EAE pathology. In addition, Bernatchez et al. (39) reported that group V $sPLA_2$ is involved in the PAF production in endothelial cells. Further studies are needed to clarify the roles of group V $sPLA_2$ in EAE lesions.

The second step of the PAF production system is acetylation of lyso-PAF to form PAF by the action of LysoPAFAT, which is critical for the stimulus-dependent formation of PAF (2–4, 12). We have previously shown that LysoPAFAT/LPCAT2 mRNA is expressed in brain, macrophages, and neutrophils (12). Likewise, we have demonstrated the constitutive expression and activity of LysoPAFAT in the SC of naive mice (Figs. 5 and 6). Since LysoPAFAT/LPCAT2 expression is mainly detected in primary cultured microglia by RT-PCR and Western blotting (Fig. 8), microglia may contribute to the production of PAF in the CNS of naive mice for maintaining brain homeostasis (Fig. 9, *left*). A number of inflammatory cells, such as T cells and macrophages, infiltrate the CNS through the broken blood-brain barrier in EAE mice. Furthermore, microglia and astrocytes are activated by cytokines produced by the infiltrating cells (40, 41). The expression and activity of LysoPAFAT were significantly elevated in SCs of EAE mice as compared with those of naive mice (Figs. 5 and 6). Because LysoPAFAT/LPCAT2 is an inducible protein, its expression might be strongly up-regulated in infiltrating macrophages and activated microglia (Fig. 9, *right*). We also have shown that LysoPAFAT activity is correlated with PLA_2 activity (Fig. 6*C*). Kalyvas and David (34) have reported that group IVA $cPLA_2$ is expressed in $CD11b^+$ cells from mice with severe symptoms of EAE. Hence, group IVA $cPLA_2$ and LysoPAFAT appear to be coexpressed in the same cells, such as macrophages/microglia, and to function coordinately in PAF synthesis. In contrast, LysoPAFAT/LPCAT2 mRNA was undetected in T cells stimulation with or without anti-CD3*e* Ab for 24 h (data not shown). These results are in accord with previous reports demonstrating that LysoPAFAT activity is present in macrophages (4, 12), but not in T cells (42). The results are also consistent with our previous report that PAF plays a dominant role in the chronic phase of EAE through the activation of macrophages/microglia (16). Taken together, LysoPAFAT induced in macrophages/microglia plays a crucial role in PAF production in EAE pathology (Fig. 9, *right*).

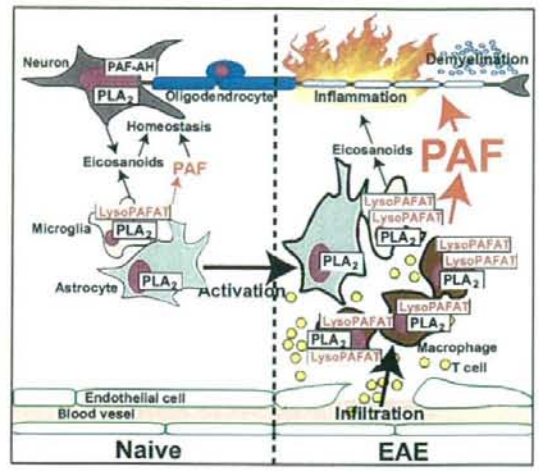

FIGURE 9. Models for PAF production in the CNS of naive mice and EAE mice. *Left*, In the CNS of naive mice, constant levels of PAF produced by microglia and astrocytes may contributes to the maintenance of CNS homeostasis. *Right*, In the CNS of EAE mice, the blood-brain barrier has been broken and inflammatory cells, such as T cells and macrophages, have infiltrated the CNS. LysoPAFAT is induced in activated microglia. Thus, robust PAF production is probably dependent on both LysoPAFAT and group IVA $cPLA_2$ coexpressed in activated macrophages and microglia.

We have measured PAF-AH activity in SCs of naive and EAE mice (Fig. 7) and found that PAF-AH activity is unchanged during the disease course of EAE. Thus, PAF may accumulate in SCs of EAE mice independently of the PAF degradation system.

Our results show that the enzyme activities in the remodeling pathway of PAF synthesis are elevated in SCs of EAE mice due to

up-regulation of group IVA cPLA$_2$ and LysoPAFAT/LPCAT2 present in macrophages and microglia (Fig. 9). Development of LysoPAFAT inhibitors may be therapeutically beneficial for the treatment of MS.

Acknowledgments

We thank Dr. N. Fukushima (Kinki University, Osaka, Japan) for advising us on the primary culturing of neurons and K. Kuniyeda (University of Tokyo, Tokyo, Japan) for valuable suggestions.

Disclosures

The authors have no financial conflict of interest.

References

1. Ishii, S., and T. Shimizu. 2000. Platelet-activating factor (PAF) receptor and genetically engineered PAF receptor mutant mice. *Prog. Lipid Res.* 39: 41–82.
2. Snyder, F. 1995. Platelet-activating factor: the biosynthetic and catabolic enzymes. *Biochem. J.* 305: 689–705.
3. Shindou, H., S. Ishii, N. Uozumi, and T. Shimizu. 2000. Roles of cytosolic phospholipase A_2 and platelet-activating factor receptor in the Ca-induced biosynthesis of PAF. *Biochem. Biophys. Res. Commun.* 271: 812–817.
4. Shindou, H., S. Ishii, M. Yamamoto, K. Takeda, S. Akira, and T. Shimizu. 2005. Priming effect of lipopolysaccharide on acetyl-coenzyme A:lyso-platelet-activating factor acetyltransferase is MyD88 and TRIF independent. *J. Immunol.* 175: 1177–1183.
5. Owen, J. S., P. R. Baker, J. T. O'Flaherty, M. J. Thomas, M. P. Samuel, R. E. Wooten, and R. L. Wykle. 2005. Stress-induced platelet-activating factor synthesis in human neutrophils. *Biochim. Biophys. Acta* 1733: 120–129.
6. Honda, Z., M. Nakamura, I. Miki, M. Minami, T. Watanabe, Y. Seyama, H. Okado, H. Toh, K. Ito, T. Miyamoto, and T. Shimizu. 1991. Cloning by functional expression of platelet-activating factor receptor from guinea-pig lung. *Nature* 349: 342–346.
7. Arai, H., H. Koizumi, J. Aoki, and K. Inoue. 2002. Platelet-activating factor acetylhydrolase (PAF-AH). *J. Biochem.* 131: 635–640.
8. Kudo, I., and M. Murakami. 2002. Phospholipase A_2 enzymes. *Prostaglandins Other Lipid Mediat.* 68–69: 3–58.
9. Kita, Y., T. Ohto, N. Uozumi, and T. Shimizu. 2006. Biochemical properties and pathophysiological roles of cytosolic phospholipase A2s. *Biochim. Biophys. Acta* 1761: 1317–1322.
10. Funk, C. D. 2001. Prostaglandins and leukotrienes: advances in eicosanoid biology. *Science* 294: 1871–1875.
11. Uozumi, N., K. Kume, T. Nagase, N. Nakatani, S. Ishii, F. Tashiro, Y. Komagata, K. Maki, K. Ikuta, Y. Ouchi, et al. 1997. Role of cytosolic phospholipase A2 in allergic response and parturition. *Nature* 390: 618–622.
12. Shindou, H., D. Hishikawa, H. Nakanishi, T. Harayama, S. Ishii, R. Taguchi, and T. Shimizu. 2007. A single enzyme catalyzes both platelet-activating factor production and membrane biogenesis of inflammatory cells: cloning and characterization of acetyl-CoA:LYSO-PAF acetyltransferase. *J. Biol. Chem.* 282: 6532–6539.
13. Pedotti, R., J. J. De Voss, L. Steinman, and S. J. Galli. 2003. Involvement of both "allergic" and "autoimmune" mechanisms in EAE, MS and other autoimmune diseases. *Trends Immunol.* 24: 479–484.
14. Steinman, L., and S. S. Zamvil. 2006. How to successfully apply animal studies in experimental allergic encephalomyelitis to research on multiple sclerosis. *Ann. Neurol.* 60: 12–21.
15. Howat, D. W., N. Chand, P. Braquet, and D. A. Willoughby. 1989. An investigation into the possible involvement of platelet activating factor in experimental allergic encephalomyelitis in rats. *Agents Actions* 27: 473–476.
16. Kihara, Y., S. Ishii, Y. Kita, A. Toda, A. Shimada, and T. Shimizu. 2005. Dual phase regulation of experimental allergic encephalomyelitis by platelet-activating factor. *J. Exp. Med.* 202: 853–863.
17. Marusic, S., M. W. Leach, J. W. Pelker, M. L. Azoitei, N. Uozumi, J. Cui, M. W. Shen, C. M. DeClercq, J. S. Miyashiro, B. A. Carito, et al. 2005. Cytosolic phospholipase A2 α-deficient mice are resistant to experimental autoimmune encephalomyelitis. *J. Exp. Med.* 202: 841–851.
18. Callea, L., M. Arese, A. Orlandini, C. Bargnani, A. Priori, and F. Bussolino. 1999. Platelet activating factor is elevated in cerebral spinal fluid and plasma of patients with relapsing-remitting multiple sclerosis. *J. Neuroimmunol.* 94: 212–221.
19. Lock, C., G. Hermans, R. Pedotti, A. Brendolan, E. Schadt, H. Garren, A. Langer-Gould, S. Strober, B. Cannella, J. Allard, et al. 2002. Gene-microarray analysis of multiple sclerosis lesions yields new targets validated in autoimmune encephalomyelitis. *Nat. Med.* 8: 500–508.
20. Pedotti, R., J. J. DeVoss, S. Youssef, D. Mitchell, J. Wedemeyer, R. Madanat, H. Garren, P. Fontoura, M. Tsai, S. J. Galli, et al. 2003. Multiple elements of the allergic arm of the immune response modulate autoimmune demyelination. *Proc. Natl. Acad. Sci. USA* 100: 1867–1872.
21. Kita, Y., T. Takahashi, N. Uozumi, L. Nallan, M. H. Gelb, and T. Shimizu. 2005. Pathway-oriented profiling of lipid mediators in macrophages. *Biochem. Biophys. Res. Commun.* 330: 898–906.
22. Kita, Y., T. Takahashi, N. Uozumi, and T. Shimizu. 2005. A multiplex quantitation method for eicosanoids and platelet-activating factor using column-switching reversed-phase liquid chromatography-tandem mass spectrometry. *Anal. Biochem.* 342: 134–143.
23. Nakanishi, H., H. Shindou, D. Hishikawa, T. Harayama, R. Ogasawara, A. Suwabe, R. Taguchi, and T. Shimizu. 2006. Cloning and characterization of mouse lung-type acyl-CoA:lysophosphatidylcholine acyltransferase 1 (LPCAT1): expression in alveolar type II cells and possible involvement in surfactant production. *J. Biol. Chem.* 281: 20140–20147.
24. Ohto, T., N. Uozumi, T. Hirabayashi, and T. Shimizu. 2005. Identification of novel cytosolic phospholipase A_2s, murine cPLA$_2\delta$, ε, and ζ, which form a gene cluster with cPLA$_2\beta$. *J. Biol. Chem.* 280: 24576–24583.
25. Kume, K., I. Waga, and T. Shimizu. 1997. Microplate chromatography assay for acetyl-CoA: lysoplatelet-activating factor acetyltransferase. *Anal. Biochem.* 246: 118–122.
26. Hattori, K., M. Hattori, H. Adachi, M. Tsujimoto, H. Arai, and K. Inoue. 1995. Purification and characterization of platelet-activating factor acetylhydrolase II from bovine liver cytosol. *J. Biol. Chem.* 270: 22308–22313.
27. Ohshima, N., S. Ishii, T. Izumi, and T. Shimizu. 2002. Receptor-dependent metabolism of platelet-activating factor in murine macrophages. *J. Biol. Chem.* 277: 9722–9727.
28. Mori, M., M. Aihara, K. Kume, M. Hamanoue, S. Kohsaka, and T. Shimizu. 1996. Predominant expression of platelet-activating factor receptor in the rat brain microglia. *J. Neurosci.* 16: 3590–3600.
29. Aihara, M., S. Ishii, K. Kume, and T. Shimizu. 2000. Interaction between neurone and microglia mediated by platelet-activating factor. *Genes Cells* 5: 397–406.
30. Tabuchi, S., K. Kume, M. Aihara, and T. Shimizu. 2000. Expression of lysophosphatidic acid receptor in rat astrocytes: mitogenic effect and expression of neurotrophic genes. *Neurochem. Res.* 25: 573–582.
31. Lucas, K. K., C. I. Svensson, X. Y. Hua, T. L. Yaksh, and E. A. Dennis. 2005. Spinal phospholipase A2 in inflammatory hyperalgesia: role of group IVA cPLA2. *Br. J. Pharmacol.* 144: 940–952.
32. Svensson, C. I., K. K. Lucas, X. Y. Hua, H. C. Powell, E. A. Dennis, and T. L. Yaksh. 2005. Spinal phospholipase A_2 in inflammatory hyperalgesia: role of the small, secretory phospholipase A_2. *Neuroscience* 133: 543–553.
33. Murakami, M., and I. Kudo. 2002. Phospholipase A_2. *J. Biochem.* 131: 285–292.
34. Kalyvas, A., and S. David. 2004. Cytosolic phospholipase A_2 plays a key role in the pathogenesis of multiple sclerosis-like disease. *Neuron* 41: 323–335.
35. Lucas, K. K., and E. A. Dennis. 2005. Distinguishing phospholipase A_2 types in biological samples by employing group-specific assays in the presence of inhibitors. *Prostaglandins Other Lipid Mediat.* 77: 235–248.
36. Pickard, R. T., B. A. Strifler, R. M. Kramer, and J. D. Sharp. 1999. Molecular cloning of two new human paralogs of 85-kDa cytosolic phospholipase A_2. *J. Biol. Chem.* 274: 8823–8831.
37. Song, C., X. J. Chang, K. M. Bean, M. S. Proia, J. L. Knopf, and R. W. Kriz. 1999. Molecular characterization of cytosolic phospholipase A_2-β. *J. Biol. Chem.* 274: 17063–17067.
38. Cunningham, T. J., L. Yao, M. Oetinger, L. Cort, E. P. Blankenhorn, and J. I. Greenstein. 2006. Secreted phospholipase A_2 activity in experimental autoimmune encephalomyelitis and multiple sclerosis. *J. Neuroinflammation* 3: 26.
39. Bernatchez, P. N., M. V. Winstead, E. A. Dennis, and M. G. Sirois. 2001. VEGF stimulation of endothelial cell PAF synthesis is mediated by group V 14 kDa secretory phospholipase A_2. *Br. J. Pharmacol.* 134: 197–205.
40. Benveniste, E. N. 1997. Role of macrophages/microglia in multiple sclerosis and experimental allergic encephalomyelitis. *J. Mol. Med.* 75: 165–173.
41. Bannerman, P., A. Hahn, A. Soulika, V. Gallo, and D. Pleasure. 2007. Astrogliosis in EAE spinal cord: derivation from radial glia, and relationships to oligodendroglia. *Glia* 55: 57–64.
42. Garcia, M. C., C. Garcia, M. A. Gijon, S. Fernandez-Gallardo, F. Mollinedo, and M. Sanchez Crespo. 1991. Metabolism of platelet-activating factor in human haematopoietic cell lines: differences between myeloid and lymphoid cells. *Biochem. J.* 273: 573–578.

The FASEB Journal article fj.08-113274. Published online September 8, 2008.
The FASEB Journal • Research Communication

Cysteinyl leukotriene 2 receptor-mediated vascular permeability *via* transendothelial vesicle transport

Michael P. W. Moos,* Jeffrey D. Mewburn,‡ Frederick W. K. Kan,§ Satoshi Ishii,‖,¶ Manabu Abe,# Kenji Sakimura,# Kyoko Noguchi,‖ Takao Shimizu,‖ and Colin D. Funk*,†,1

*Department of Physiology, †Department of Biochemistry, ‡Division of Cancer Biology and Genetics, Cancer Research Institute, and §Department of Anatomy and Cell Biology, Queen's University, Kingston, Ontario, Canada; ‖Department of Biochemistry and Molecular Biology, Faculty of Medicine, University of Tokyo, Tokyo, Japan; ¶Precursory Research for Embryonic Science and Technology (PRESTO), Japan Science and Technology Agency, Tokyo, Japan; and #Department of Cellular Neurobiology, Brain Research Institute, Niigata University, Niigata City, Japan

ABSTRACT **Cysteinyl leukotrienes (CysLTs) are potent mediators of inflammation synthesized by the concerted actions of 5-lipoxygenase (5-LO), 5-LO-activating protein (FLAP), leukotriene C_4 synthase, and additional downstream enzymes, starting with arachidonic acid substrate. CysLTs produced by macrophages, eosinophils, mast cells, and other inflammatory cells activate 3 different high-affinity CysLT receptors: $CysLT_1R$, $CysLT_2R$, and GPR 17. We sought to investigate vascular sites of $CysLT_2R$ expression and the role and mechanism of this receptor in mediating vascular permeability events. Vascular expression of $CysLT_2R$ was investigated by reporter gene expression in a novel $CysLT_2R$ deficient-LacZ mouse model. $CysLT_2R$ was expressed in small, but not large, vessels in mouse brain, bladder, skin, and cremaster muscle. Intravital, in addition to confocal and electron, microscopy investigations using FITC-labeled albumin in cremaster postcapillary venule preparations indicated rapid CysLT-mediated permeability, which was blocked by application of BAY-u9773, a dual $CysLT_1R/CysLT_2R$ antagonist or by $CysLT_2R$ deficiency. Endothelial human $CysLT_2R$ overexpression in mice exacerbated vascular leakage even in the absence of exogenous ligand. The enhanced vascular permeability mediated by $CysLT_2R$ takes place *via* a transendothelial vesicle transport mechanism as opposed to a paracellular route and is controlled *via* Ca^{2+} signaling. Our results reveal that $CysLT_2R$ can mediate inflammatory reactions in a vascular bed-specific manner by altering transendothelial vesicle transport-based vascular permeability.—Moos, M. P. W., Mewburn, J. D., Kan, F. W. K., Ishii, S., Abe, M., Sakimura, K., Noguchi, K., Shimizu, T., Funk, C. D. Cysteinyl leukotriene 2 receptor-mediated vascular permeability *via* transendothelial vesicle transport. *FASEB J.* 23, 000–000 (2009)**

Key Words: inflammation · intravital microscopy · transgenic mice · caveolae

INFLAMMATION, THE FUNDAMENTAL response of blood vessels and adjacent tissues to injury or abnormal stimulation caused by physical, chemical, or biological agents, is a dynamic complex of cytological and molecular events. The cardinal signs of inflammation—redness, warmth, swelling, and pain—are sometimes accompanied by inhibition or loss of function. Whereas warmth and redness are mainly due to increased blood flow in the affected tissue as a result of vasodilation, swelling is based on enhanced vascular permeability that leads to plasma extravasation and results in edema. This enhanced vascular permeability allows emigration of leukocytes and inflammatory mediators to sites of tissue injury as part of the acute response in tissue healing (1). The local increase in microvascular permeability due to disruption of endothelial integrity after surgery can contribute to death by multiple organ dysfunction syndrome (2). Chronic inflammation that causes protracted vascular hyperpermeability and consequent plasma leakage may be responsible for some of the pathophysiological sequelae in atherosclerosis, arthritis, asthma, and proliferative vitreoretinopathy (3).

Cysteinyl leukotrienes (CysLTs) are among the most active known inflammatory mediators (4). The key enzyme for the synthesis of leukotrienes is 5-lipoxygenase (5-LO), which in combination with the 5-LO-activating protein (FLAP) transforms arachidonic acid into leukotriene A_4, which is further modified by leukotriene C_4 synthase (LTC_4S) to leukotriene (LT) C_4. LTC_4 can be further metabolized to LTD_4 and LTE_4. CysLTs bind to 3 different receptors of the G protein-coupled receptor superfamily: cysteinyl leukotriene receptor subtype 1 ($CysLT_1R$), cysteinyl leukotriene receptor subtype 2 ($CysLT_2R$), and the recently characterized GPR17 (4, 5). The distinct expression patterns of the receptors reveal that they are likely to play separate functions and perhaps be implicated in different aspects of the inflammatory response and cardiovascular

[1] Correspondence: Department of Physiology, 433 Botterell Hall, Stuart St., Queen's University, Kingston, ON K7L 3N6, Canada. E-mail: funkc@queensu.ca

doi: 10.1096/fj.08-113274

0892-6638/09/0023-0001 © FASEB

disease. There has been recent widespread, heightened interest in the 5-LO/leukotriene pathway with respect to cardiovascular inflammation in atherosclerosis, myocardial infarction, and stroke (6–9). Whereas $CysLT_1R$ has been studied in great detail in relation to asthma and other inflammatory disorders (6), our knowledge of $CysLT_2R$ functions is still rather limited, which is in part due to the lack of a specific receptor antagonist.

Recent data from our laboratory and others have implicated $CysLT_2R$ in vascular inflammatory and permeability events in response to leukotriene administration in acute inflammation and in myocardial ischemia/reperfusion injury (10–12). These studies were carried out with $CysLT_2R$ deficient mice (12), as well as with mice overexpressing human $CysLT_2R$ in vascular endothelium (10), a site where $CysLT_2R$ expression has been observed (11, 13). However, much remains to be learned about the mechanism of these events.

The semipermeable characteristic of the endothelium is crucial for establishing the transendothelial protein gradient (the colloid osmotic gradient) that is required for tissue fluid homeostasis (14). Disruption of the endothelial cell barrier results in increased permeability and vascular leak, and endothelial cells are able to dynamically regulate so-called paracellular and transcellular pathways for transport of plasma proteins, solutes, and liquid (14). Interendothelial junctions consist of a complex array of proteins in series with extracellular matrix constituents that serve to limit the transport of albumin and other plasma proteins by paracellular mechanisms. Transcellular regulation can take place at the level of caveolae, the vesicular carriers filled with receptor-bound and unbound free solutes, or *via* transendothelial channels, fluid phase vesicle, and receptor-mediated transport. Here, we have studied the vascular bed-specific expression pattern of $CysLT_2R$ using a novel $CysLT_2R$ knockout mouse strain in which the reporter LacZ gene has been integrated, as well as the impact of $CysLT_2R$ stimulation on the mechanism of vascular permeability using intravital microscopy.

MATERIALS AND METHODS

Animals

The generation of EC-$CysLT_2R$ transgenic mice has been described previously (10). These mice express 7 copies of the human $CysLT_2R$ coding region under control of the Tie2 promoter/enhancer, integrated in a gene-sparse region of chromosome 6. Hemizygous mice were continuously backcrossed with C57BL/6 mice to obtain equal numbers of transgenic (TG) and wild-type (WT) littermates. $CysLT_2R$ deficient-LacZ mice (KO) were generated by standard gene targeting procedures using C57BL/6 embryonic stem cells (unpublished results) Embryos heterozygous for the genetic modification were transferred from Japan and revived at Queen's University. Littermates of heterozygous offspring (all on a C57BL/6 genetic background) were used in these studies. Sequencing of the *Cysltr2* gene verified that the LacZ coding region was in frame with the start codon of a truncated $CysLT_2R$ open-reading frame that yields a genetic *Cysltr2* disruption and allows use of X-Gal staining as a reporter for native sites of $CysLT_2R$ expression.

Investigation of $CysLT_2R$ expression using the reporter LacZ

Tissues were dissected and fixed in 2% paraformaldehyde/0.2% glutaraldehyde on ice for 30 min. LacZ staining was carried out overnight at 37°C in phosphate-buffered saline (PBS) containing 2 mM $MgCl_2$, 5 mM potassium ferrocyanide trihydrate, 5 mM potassium ferricyanide crystalline, 1 mg/ml X-Gal, and 2.5% dimethyl sulfoxide (DMSO).

Experimental intravital microscopy procedures

Mice were anesthetized with ketamine (150 mg/kg) and xylazine (10 mg/kg), and a catheter was placed in the right jugular vein. The cremaster muscle covering the right testicle was prepared as described in detail elsewhere (15). For Ca^{2+} signaling-related experiments, the cremaster muscle was superfused with Ca^{2+}-free PBS. Microscopic evaluation of postcapillary venules (~17 μm diameter) was recorded throughout the experiment on S-VHS video tape for subsequent data analysis. Initially, bright field images were recorded for 5 min, and blood velocity in the vessel was measured. Fluorescein isothiocyanate (FITC) -labeled albumin (25 mg/kg body weight) was injected *via* the catheter, and fluorescence in the preparation was recorded for at least 5 min. CysLTs (LTC_4 and LTD_4, both at 5 μM) or BAY-u9773 (1 μM) were administered to the superfused vessel. After 5 min, a second treatment with CysLTs or BAY-u9773 was carried out, followed by recording for at least 5 min.

The vessel diameter and blood velocity were measured for each experiment prior to and after treatments but were not modified by any of the different experimental parameters.

To block Ca^{2+} signaling, we added the acetoxymethyl form of the Ca^{2+}-chelator BAPTA (BAPTA-AM; 10 μM) (16) to the suffusion medium and preincubated the cremaster muscle for 15 min before injecting FITC-labeled albumin and prior to CysLT stimulation. In separate experiments, thapsigargin (30 μM final concentration), an inhibitor of the sarco/endoplasmic reticulum Ca^{2+}-ATPase (SERCA), was applied to discharge intracellular Ca^{2+} stores to generate a steady Ca^{2+} signal (17, 18).

To block caveolae/lipid rafts and thereby transcellular vesicle transport, 20 mM methyl-beta-cyclodextrin (MBCD) was added to the suffusate. The cremaster muscle was preincubated for 15 min, followed by CysLT and BAY-u9773 treatment, as described above.

Quantification of vascular permeability

To quantify vascular permeability of postcapillary venules in the cremaster muscle, digital images were stored every 20 s throughout fluorescence recording. The mean fluorescence intensity for each image was measured (gray level range from 0 (black) to 255 (white)).

We calculated a linear function $f(x) = mx + n$ describing the change in fluorescence intensity m over time x for every stage of the experiment (pretreatment and posttreatment). The parameter LIFT (leakage intensity factor for tissues) was calculated as the first equation of this linear function. This LIFT parameter describes the slope of a linear function representing the changes in fluorescence intensity in the tissue over time and is therefore a measure for vascular permeability.

Quantification of FITC-albumin accumulation sites

Sites of FITC-labeled albumin accumulation were initially recorded with a SonyDXC-390m3 CCD color video camera (Sony, Tokyo, Japan). Subsequently, we used a digital camera (ORCA-ER C4742-80-12AG, Hamamatsu Photonics K.K., Hamamatsu City, Japan) to determine the number of accumulating sites at greater resolution and sensitivity. Sites of accumulation of FITC-labeled albumin were determined based on the histogram of the entire image and were counted with Image Pro software (Media Cybernetics, Bethesda, MD, USA).

To allay concern that FITC-labeled albumin accumulation within cells (see Results) does not influence vascular permeability measurements that are based on total brightness of the recorded images, we modeled the effect by using a total black picture (gray level 0) on which 15 white spots (gray level 255 U) sized at 100 pixels were added to represent FITC-albumin accumulation. The change in total brightness (0.28 U) represented by this procedure is comparable to a 12 s measurement from unstimulated WT cremaster muscle preparations. To exaggerate this process we marked the periphery of a typical venule outline white, which caused a brightness change (1.36 U) that resembles only 11 s of recorded leakage from CysLT-stimulated WT preparations. Since the permeability measurements and LIFT parameter were calculated based on a 5 min observation, the contribution of FITC-albumin accumulation sites to LIFT represents less than 3.6% and was therefore regarded as negligible.

Confocal microscopy

Cremaster muscles were collected after intravital microscopy experiments and immediately fixed in 2% paraformaldehyde/0.2% glutaraldehyde on ice for 30 min. The tissue was embedded in Tissue-Tek (Sakura Finetek, Torrance, CA, USA). Cryosections (10 μm) were cut and labeled with pan-endothelial cell antigen antibody MECA-32 (BD Pharmingen, San Diego, CA) and Texas Red conjugated goat anti-rat immunoglobulin G (IgG). Sections were examined using a Leica TCS SP2 multi photon confocal laser scanning microscope (Leica Microsystems, Wetzlar, Germany).

Electron microscopy

For electron microscopic examination of transcytotic vesicles in blood vessels of the cremaster muscle, we followed intravital microscopy procedures as described above. The cremaster muscle was excised and fixed immediately by immersion in 2.5% glutaraldehyde in 0.1 M cacodylate buffer, pH 7.4. After 2 h at 4°C, the tissue samples were washed 3 times with PBS and then trimmed into small pieces for Epon embedding (Epon 812), as described previously (19). One-micrometer-thick sections were first examined by light microscopy in order to locate the area of interest, after which Epon thin sections were cut with a diamond knife on a LKB ultramicrotome and mounted on copper grids. After counterstaining with uranyl acetate and lead citrate solutions, the sections were examined on a Hitachi 7000 electron microscope operated at 75 kV. In randomly taken pictures of postcapillary venules, the area of endothelial cells was measured and the vesicles inside were counted.

Cell culture

Murine b-end.3 endothelial cells were kindly provided by Dr. Yves St. Pierre (University of Quebec, Quebec, QC, Canada). Cells were tested for $CysLT_1R$ (CAGGAGCCCTGTGAATGGAG, GTGGCCACTGTTCTTATGTTG) and $CysLT_2R$ (CGTTCACCAGAAGCAGGGC, CTGAGTGTGGTGCGTTTCCTG) expression by polymerase chain reaction. Cells were subsequently transfected with pcDNA3-huCysLT2R vector (13) and selected with Geneticin (Invitrogen, Carlsbad, CA, USA) to generate stable $huCysLT_2R$ overexpressing cells. Prior to experiments, cells were incubated for 5 min in PBS, followed by addition of FITC-albumin (1.33 μg/ml in PBS), LTC_4/LTD_4 (5 μM in FITC-albumin/PBS), or BAY-u9773 (1 μM in FITC-albumin/PBS). Cells were washed with PBS and fixed in 2% paraformaldehyde/0.2% glutaraldehyde and examined by fluorescence microscopy.

Statistical analysis

For each experimental group, the mean and SE were calculated. To compare groups, we performed 2-sided t tests for independent samples. $P < 0.05$ was considered a statistically significant difference.

RESULTS

$CysLT_2R$ expression in vasculature

Using a novel $CysLT_2R$ deficient-LacZ mouse strain in which the LacZ reporter gene is driven by the *Cysltr2* gene promoter (unpublished results), we assessed vascular $CysLT_2R$ expression with X-Gal blue staining in a variety of organs. No $CysLT_2R$ expression could be detected in the vasculature of lung, intestines, and liver. On the other hand, a few discrete areas of positive staining were detected in blood vessels of the heart and in cardiac tissue after myocardial ischemia/reperfusion injury, and also in vessels of the muscular body wall and diaphragm (11 and data not shown). However, in organs including the bladder, brain/spinal cord, skin, ear, and the cremaster muscle surrounding the testis, strong staining in small vessels was evident, whereas the larger blood vessels were negative (**Fig. 1**). Section analysis revealed staining in the microvasculature within endothelial cells. These results indicate that $CysLT_2R$ expression in the vasculature occurs within the endothelium and is dependent on the organ and vessel size.

Intravital microscopy to assess role of $CysLT_2R$ in vascular permeability

We have recently shown that CysLTs evoke $CysLT_2R$-mediated vascular permeability responses in the ear and in the heart after ischemia/reperfusion injury of TG mice that overexpress human $CysLT_2R$ in vascular endothelium (10, 11). To visualize this process and to assess the importance of endogenous $CysLT_2R$ and CysLTs, we undertook an intravital microscopy study with KO mice as well as with TG and WT C57BL/6 mice using the well-established cremaster muscle preparation. We observed strong endogenous small-vessel $CysLT_2R$ expression (Fig. 1). Fluorescence intensity measurements in vascular preparations from WT and KO mice after administration of FITC-labeled albumin

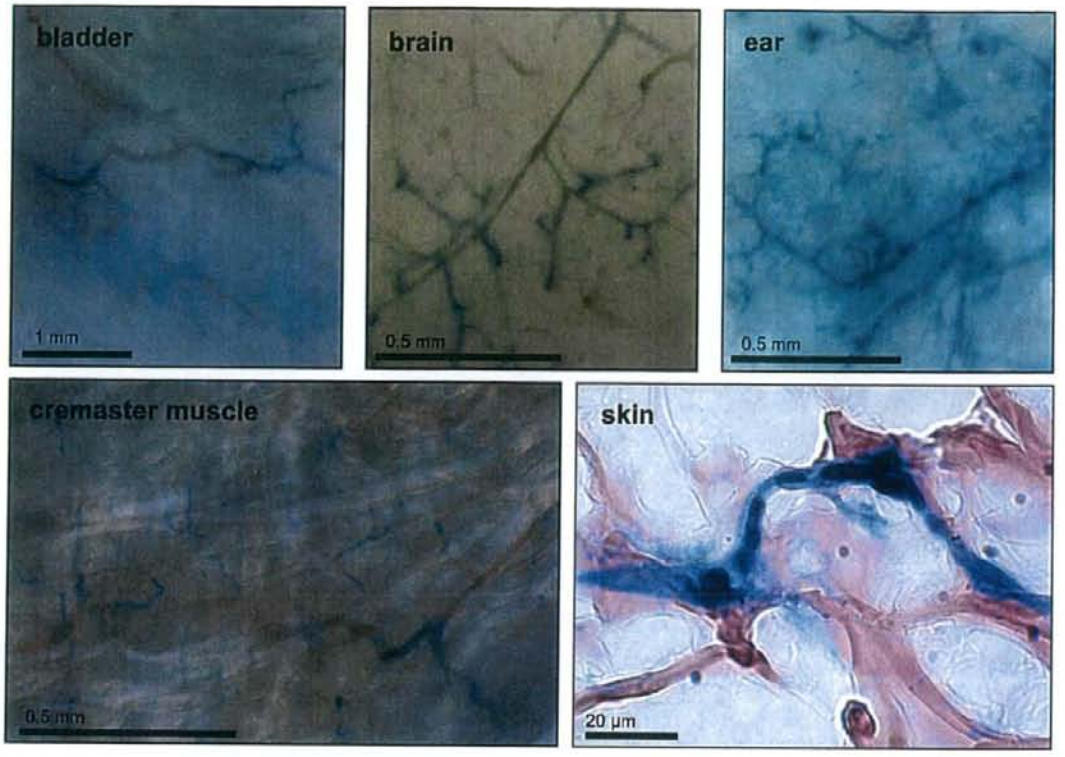

Figure 1. Sites of vascular $CysLT_2R$ expression in various organs using surrogate LacZ reporter gene expression driven by the *Cysltr2* gene promoter. Small vessels within the bladder (top left panel), brain (top middle panel), ear (top right panel), and cremaster muscle (bottom left panel) demonstrate strong X-gal blue positivity indicating $CysLT_2R$ expression, whereas larger blood vessels in these organs show little or no staining. Sectioning of dorsal skin (bottom right panel) reveals strong expression of $CysLT_2R$ in the microvascular endothelium.

revealed a stable pattern, indicating minimal vascular permeability (**Figs. 2** and **3**) that did not change within 20 min in control experiments. Superfusion of the tissue with CysLTs (5 µM each LTC_4/LTD_4) evoked a strong and rapid increase in vascular permeability over 5–15 min, as measured by increasing extravascular fluorescence intensity in WT mice. However, no effect was observed in KO mouse preparations (Figs. 2 and 3). In contrast, TG mice showed evidence, even without exogenous CysLT administration, of increased vascular permeability shortly after FITC-albumin injection, attaining greater than 50% the level observed in CysLT-stimulated WT mice (Figs. 2 and 3). The vessels visualized in these experiments had the same diameter range (WT, 16.9±4.4 µm, n=21; TG, 17.2±2.3 µm, n=22).

Vascular leakage of FITC-albumin by CysLTs could be quenched rapidly to a level where changes in fluorescence intensity are no longer detectable by application of the dual $CysLT_1R/CysLT_2R$ antagonist BAY-u9773 (1 µM; Fig. 3). This effect was observed in vascular preparations from TG and WT mice with and without preceding CysLT stimulation (Fig. 3). BAY-u9773 treatment, on the other hand, had no visible effect on vascular permeability as measured by fluorescence intensity in the vasculature of KO mice (Fig. 3).

In contrast to the high permeability observed in the right cremaster muscle vascular preparation of live TG mice, no signs of immediate vascular permeability (FITC-albumin leakage or FITC-albumin accumulating sites; see below) could be seen in the left cremaster muscle, which was prepared after euthanization to eliminate blood flow- or blood pressure-related effects. This suggests that one possibility for the observed strong vascular permeability response in TG mice in the absence of exogenous ligands was caused by endogenous CysLTs released during the initial surgical intervention interacting with enhanced numbers of $CysLT_2R$ in the endothelium.

$CysLT_2R$ challenge with BAY-u9773 subsequent to vascular permeability elevation leads to endothelial cell accumulation of FITC-albumin

Besides the obvious vascular leakage of FITC-albumin into the extravascular tissue of TG and WT mice, there was evidence for distinct FITC-albumin accumulating

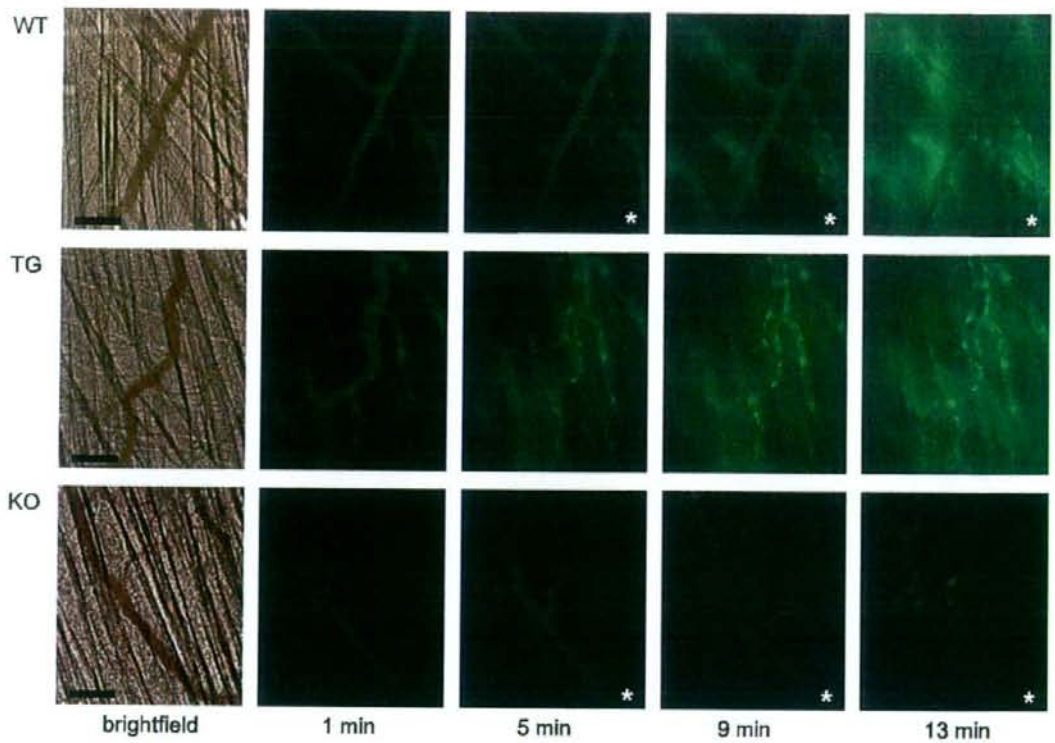

Figure 2. Intravital microscopy recordings of vascular leakage in cremaster muscle postcapillary venules using FITC-labeled albumin. One representative mouse cremaster muscle preparation from each of 3 groups expressing normal (WT, top panels), elevated (TG, middle panels), and no (KO, bottom panels) $CysLT_2R$ are depicted ($n \geq 8$). Leftmost panels show brightfield images; other panels in each row show fluorescence recordings at indicated time points after administration of FITC-labeled albumin *via* a jugular vein catheter. Asterisks indicate period of CysLT superfusion of WT and KO preparations. Scale bars = 50 μm.

bright fluorescent sites (Figs. 2 and **4*A***). These sites are most evident where the leakage of FITC-albumin into the surrounding tissue was initiated and can be used as a marker for number of leakage sites (20). The number of these bright fluorescent sites per unit area was significantly higher in vascular preparations from TG mice compared to WT mice in the absence of exogenous CysLT administration (Fig. 2 and data not shown). CysLT stimulation evoked not only an increase in vascular leakage in WT mice (Figs. 3 and **5**), but also caused a significant increase in the number of these bright accumulation sites. Challenge with BAY-u9773 led to a further significantly increased number of FITC-albumin accumulation sites in both WT and TG mice. These sites are localized in distinct regions on the inner vessel wall, where they can cover almost the whole vessel after BAY-u9773 treatment, as shown in Fig. 4*A*. The location and pattern of the FITC-albumin bright sites implies that endothelial cells after $CysLT_2R$ stimulation initiate vascular permeability by a transcellular pathway rather than at interendothelial gap junctions. These results also indicate that $CysLT_2R$ challenge with BAY-u9773 restores the barrier function of the endothelium by blocking exocytosis at the abluminal site of the endothelium which is shown by an increase in accumulation of albumin at sites of prior high vascular permeability (Fig. 5). This hypothesis is supported by the fact that when vascular preparations from WT and TG mice were first pretreated with BAY-u9773, followed by subsequent stimulation with CysLTs, there was a sudden increase in fluorescence intensity. Therefore, after CysLT treatment, stored fluorescent albumin within endothelial cells was suddenly released. This reaction was quite unique and could not be reproduced by CysLT treatment alone or by a second BAY-u9773 addition (data not shown).

Examining this in further detail, confocal laser scanning images revealed accumulation of FITC-albumin within endothelial cells (positive for the pan-endothelial cell marker Meca-32) of blood vessels after CysLT stimulation (Fig. 4*B*), indicating transcellular transport. Moreover, electron microscopy analysis of CysLT- and BAY-u9773-treated postcapillary venules revealed a significantly increased number of vesicles inside the endothelium compared to unstimulated venules (**Fig. 6**), suggesting an increase in vesicle formation and/or transport in response to CysLT stimulation.

To mimic the *in vivo* setting within endothelial cells

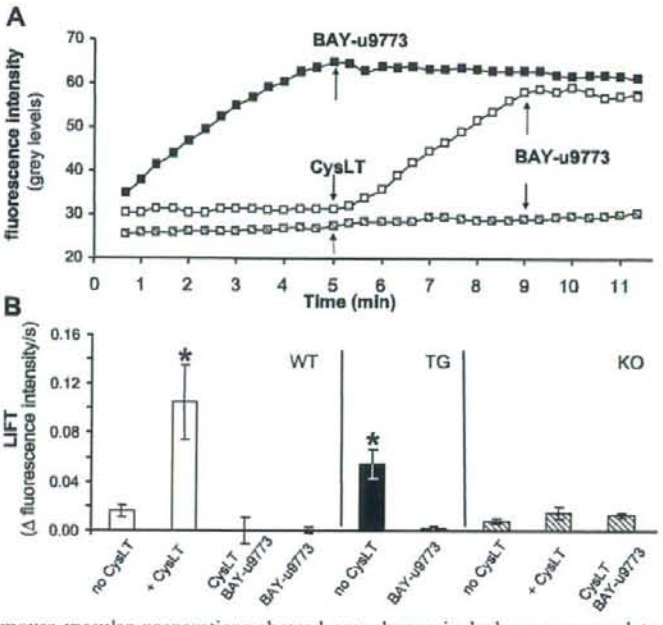

Figure 3. $CysLT_2R$ mediates vascular permeability in cremaster muscle postcapillary venules. *A*) Representative measurements of fluorescence intensity in cremaster muscle preparations from WT (open boxes), TG (filled boxes), and KO (striped boxes) mice used to calculate FITC-albumin leakage. After i.v. FITC-albumin administration, WT and KO mouse preparations were treated after 5 min with LTC_4/LTD_4 (CysLT) superfusion and 4 min later with the dual $CysLT_1R/CysLT_2R$ antagonist BAY-u9773. Autogenous leakage in TG preparations was blocked by treatment with BAY-u9773 after 5 min. Neither CysLTs nor BAY-u9773 treatment of KO mouse preparations caused changes in vascular leakage. *B*) LIFT parameter (mean+SE; see Materials and Methods) was calculated for several experimental conditions: no CysLT treatment (n=17, WT; n=14, TG; n=8, KO); with CysLT (5 μM) stimulation (n=10, WT; n=8, KO); after BAY-u9773 (1 μM) with preceding CysLT stimulation (n=6, WT; n=8, KO); or only with BAY-u9773 treatment (n=6, WT and TG). LIFT is significantly higher (P<0.01) in CysLT-stimulated WT and unstimulated TG vascular preparations compared to the other groups. BAY-u9773 treatment reduced LIFT to almost 0 in WT and TG mice, whereas neither CysLT nor BAY-u9773 treatment of KO mouse vascular preparations showed any change in leakage compared to untreated conditions.

of TG mice in a tissue culture model, b-end.3 mouse endothelial cells were permanently transfected with human $CysLT_2R$ ($CysLT_2R$ b-end.3) and tested for fluorescent albumin accumulation (Fig. 4*C*). We determined that native endothelial cell line b-end.3 expresses neither $CysLT_1R$ nor $CysLT_2R$, and these cells do not accumulate FITC-albumin even after stimulation with CysLTs or BAY-u9773. $CysLT_2R$ b-end.3 cells, on the other hand, showed a significant number of labeled-albumin accumulating cells after treatment with CysLTs or BAY-u9773. Together, these data indicate that $CysLT_2R$ modulation leads to endothelial cell albumin uptake.

$CysLT_2R$-induced vascular permeability is mediated by Ca^{2+} signaling

$CysLT_2R$ stimulation in endothelial cells has been linked to oscillating calcium signals of unknown functional significance (21). The inhibition of intracellular Ca^{2+} signals by BAPTA prevented enhanced vascular permeability elicited by CysLT stimulation in WT cremaster muscle preparations (Fig. 5). This indicates that intracellular Ca^{2+} signals are essential for $CysLT_2R$-regulated vascular permeability.

Thapsigargin causes the release of Ca^{2+} from intracellular stores by blocking SERCA, thereby creating a

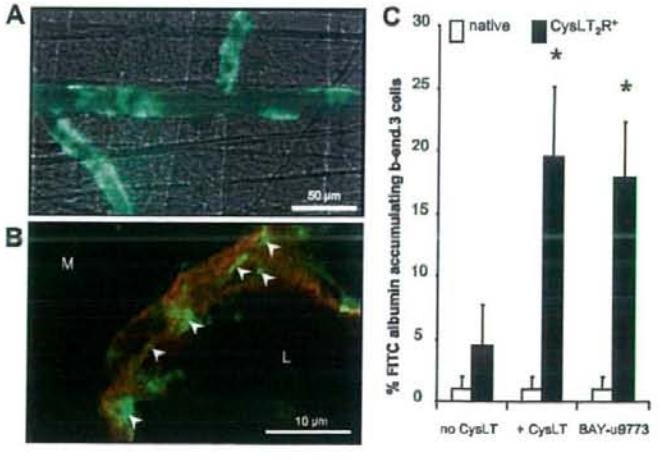

Figure 4. FITC-labeled albumin accumulation *in vivo* and *in vitro* affected by $CysLT_2R$ activation and BAY-u9773. *A*) Merge of fluorescence and phase-contrast images of postcapillary venules from a TG mouse revealing FITC-albumin accumulation along the inner vessel wall after BAY-u9773 treatment. *B*) Confocal laser scanning image showing FITC-labeled albumin (green) inside Meca32/Texas Red-labeled endothelium (red), blood vessel lumen (L), and surrounding muscular tissue (M); white arrowheads point to intracellular FITC-albumin accumulation. *C*) FITC-albumin accumulation in native and human $CysLT_2R$ transfected b-end.3 murine endothelial cells was examined after stimulation with CysLTs or BAY-u9773. While native cells, which do not express CysLT receptors, fail to accumulate FITC-albumin, the transfected cells do so after both treatments. *$P < 0.05$ *vs.* native cells; $n = 3$.

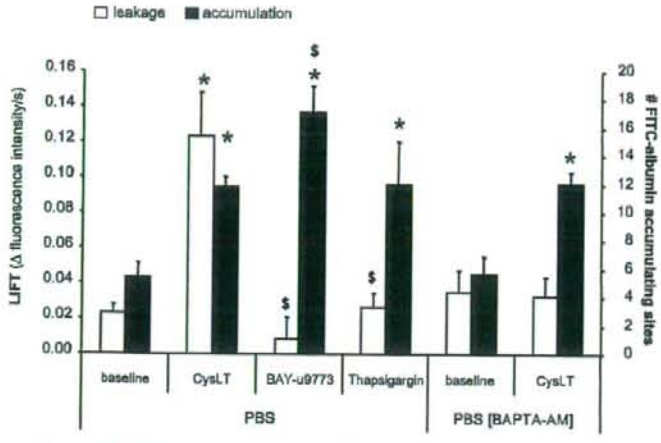

Figure 5. Endothelial vascular leakage sites affected by $CysLT_2R$-activated Ca^{2+} signaling. Vascular permeability (LIFT; white bars) was calculated and FITC-labeled albumin accumulating sites were counted (black bars) in WT cremaster muscle preparations for several experimental conditions: WT mice without treatment (n=17 LIFT/n=7 hot spots); after stimulation with LTC_4/LTD_4 (n=12/n=4); LTC_4/LTD_4-prestimulated preparations followed by BAY-u9773 (n=7/n=3); treatment with thapsigargin (n=5/n=3); and BAPTA preincubation with (n=7/n=3) and without LTC_4/LTD_4 stimulation (n=6/n=3). CysLT-induced heightened vascular permeability is inhibited by BAY-u9773 and the Ca^{2+} chelator BAPTA. The steady Ca^{2+} signal released by thapsigargin does not induce vascular permeability alterations but leads to FITC-albumin accumulation in the endothelium. FITC-labeled albumin accumulation is triggered by CysLT stimulation regardless of BAPTA treatment and can be further increased with the dual $CysLT_1R$/$CysLT_2R$ antagonist BAY-u9773. Data are means ± SE; $^*P < 0.05$ *vs.* baseline; $^\$P < 0.05$ *vs.* CysLT stimulation.

steady Ca^{2+} signal. However, in these experiments (Fig. 5), treatment with thapsigargin did not lead to an increase of vascular permeability, indicating that a steady Ca^{2+} signal is not sufficient to provoke vascular leakage. While thapsigargin did not elevate vascular permeability, its application led to an increased number of FITC-labeled albumin accumulation sites in the absence of CysLT administration. This signifies that thapsigargin may induce endothelial luminal endocytosis, but not abluminal exocytosis. The fact that BAPTA blocked vascular permeability but only marginally influenced the number of CysLT-stimulated FITC-albumin accumulation sites (Fig. 5) reveals that the Ca^{2+}-buffering capacity of BAPTA is important for setting weaker oscillating Ca^{2+} signals, as described previously in *Xenopus* melanotropes (22), which might influence exocytosis of labeled-albumin from the vascular endothelial cells into the extravascular space.

Blockade of caveolae and subsequent vesicle formation with MBCD attenuates transcytosis of albumin in response to CysLT stimulation

Caveolae are known to transport albumin and other plasma proteins across the endothelium, and it is at these sites that vesicles are derived for transcytosis (14). Inhibition of caveolae/lipid rafts by application of MBCD resulted in significantly decreased baseline vascular permeability (LIFT=0.002±0.002; n=8; P<0.01, +MBCD *vs.* −MBCD) and a significantly delayed response to CysLT stimulation (**Fig. 7*B***). The CysLT-induced increase of vascular permeability (LIFT=0.121±0.018; n=8) could not be inhibited by application of BAY-u9773 (LIFT=0.110±0.027; n=4), as observed in cremaster muscle preparations not treated with MBCD (Fig. 7*A*; compare Fig. 3). However, the bright fluorescent accumulation of albumin within endothelial cells was blocked by MBCD (Fig. 7*C*). These results

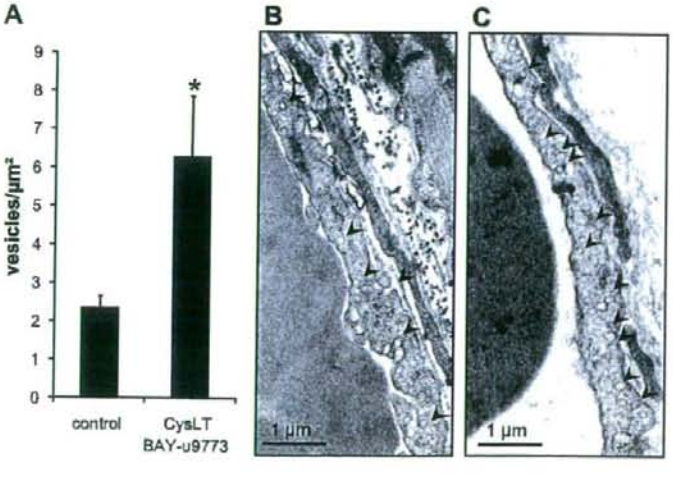

Figure 6. $CysLT_2R$-mediated transendothelial vesicles. *A*) Vesicles per unit area in endothelial cells counted on electron microscopy images of cremaster muscle sections taken after intravital microscopy experiments treated with CysLT and BAY-u9773. Contralateral untreated cremaster muscle was used as a control. CysLT/BAY-u9773-treated cremaster muscle sections show a significantly increased number of vesicles compared to controls. $^*P < 0.05$; n = 8. *B, C*) Representative electron microscopy images of a section from a control (*B*) and a CysLT/BAY-u9773-treated cremaster muscle (*C*) with vessel lumen toward the left. Black arrowheads point to vesicles in the endothelial cell.

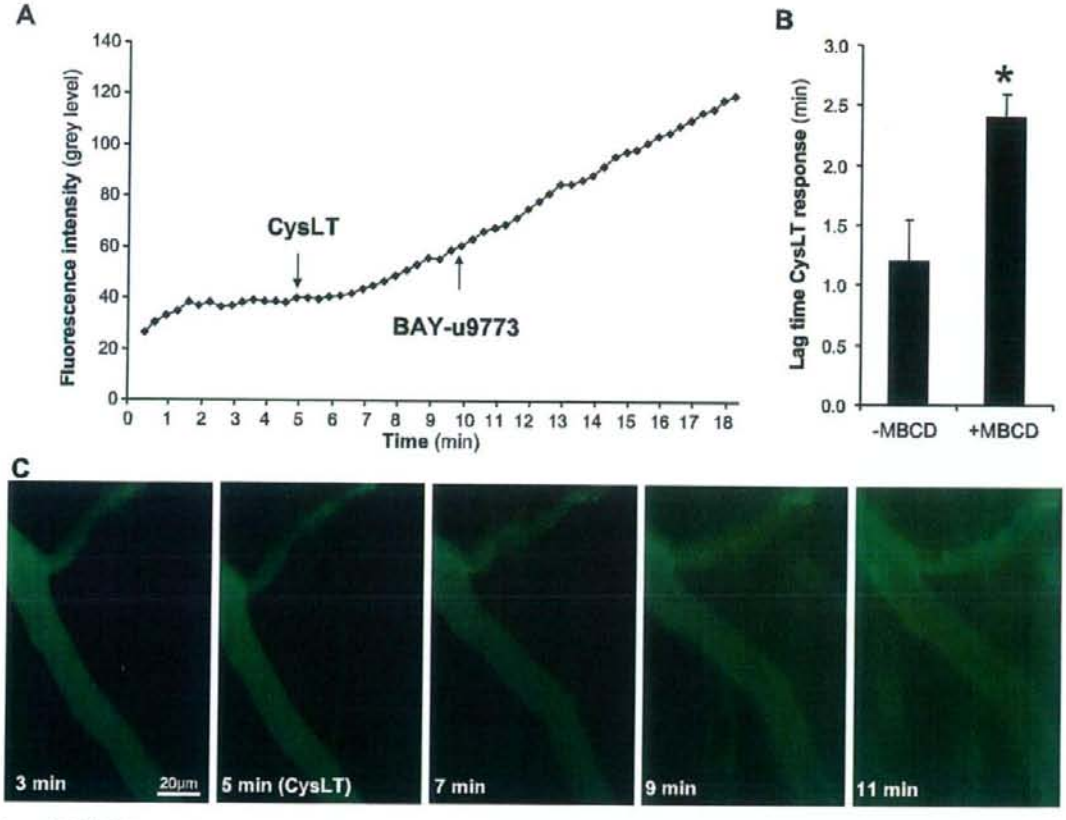

Figure 7. Inhibition of caveolae with MBCD causes a time-delayed vascular permeability response without FITC-albumin accumulation in the vessel wall. *A*) Representative measurements of fluorescence intensity in a cremaster muscle preparation from a WT mouse preincubated for 15 min with MBCD. After i.v. FITC-albumin administration, CysLTs stimulate an increase of fluorescence with a lag time of 2 min that is not influenced by subsequent application of BAY-u9773. *B*) CysLT response lag time for WT mice cremaster muscles with (+) MBCD preincubation is significantly increased compared to non-MBCD treated (−) mice. $n = 6$; $^*P < 0.05$. *C*) Representative series of images from an MBCD-pretreated cremaster muscle. Leakage starts 2 min after application of CysLT without establishing FITC-albumin accumulation sites within the vessel wall.

indicate that blockade of caveolae inhibits transcytosis but may activate a compensatory paracellular transport mechanism, as recognized in caveolin-1 null mice (23).

DISCUSSION

The first analysis of $CysLT_2R$ KO mice (12) and TG mice overexpressing human $CysLT_2R$ in vascular endothelium (10) indicated a potential role for $CysLT_2R$ activation to increase vascular permeability. In the present study, we explored this facet in greater detail by means of intravital/confocal/electron microscopy imaging combined with a determination of vascular sites of $CysLT_2R$ expression. Our findings indicate an organ and blood vessel specificity of $CysLT_2R$ expression and that in cremaster muscle postcapillary venules, $CysLT_2R$ is the major leukotriene receptor subtype involved in the control of vascular permeability through a transcellular transport pathway. The fact that the permeability response in this vascular bed was absent in $CysLT_2R$ KO mice indicates that neither $CysLT_1R$ nor the newly discovered CysLT receptor known as GPR17 (5) participate in this activity. These results reveal a key role for $CysLT_2R$ in vascular responses to injury, such as that observed after myocardial infarction/reperfusion, as we have reported recently (11).

In the cremaster muscle preparation, TG mice displayed enhanced vascular permeability without exogenous ligand administration, whereas in WT mice this could only be observed after stimulation with CysLTs. These observations suggest that TG mice would develop massive edema, which has not been observed previously. In ear inflammation models, either exogenous CysLT administration was required (direct model) or an induction of CysLT synthesis was necessary (passive cutaneous anaphylaxis model) (10). No signs of enhanced vascular permeability/FITC-albumin leakage or FITC-albumin accumulating leakage sites could be observed in the contralateral (left) cremaster muscle of WT or TG mice immediately after euthanization. This

leads us to surmise that in TG mice the observed hyperpermeability vascular response might be due to the surgical intervention; presumably, low levels of CysLT are produced by resident tissue macrophages and/or mast cells during preparation of the cremaster muscle on the microscope stage. Because of the enhanced numbers of $CysLT_2R$ binding sites within the vascular endothelium of TG mice, they are likely more sensitive to CysLTs and therefore respond to endogenous CysLTs to a much greater degree than WT mice. An alternative, albeit less likely, interpretation is that the overexpressed $CysLT_2R$ is constitutively active in some vascular beds, although the ligand-independent activation of GPCRs and constitutive activity *in vivo* have been difficult to verify (24).

FITC-albumin extravasation from the venules is initiated and takes place at certain "hot spots" of fluorescence accumulation called "leaky sites" by Huang *et al.* (20). In our studies, these sites were observed in discrete regions throughout the endothelium. They have been observed by intravital microscopy in response to burns (20), platelet-activating factor/leukotriene B_4 (25), and CysLTs (herein), but not in response to many other stimuli, such as histamine (26), tumor necrosis factor α (27), and homocysteine (28). Electron microscopy observations of albumin extravasation have revealed that it is mediated mainly by transcellular vesicle transport (14, 29 and Fig. 6). Furthermore, pinocytotic vesicular transport appears to be a primary means by which luminal to abluminal transport occurs in response to bradykinin/LTC_4 stimulation to enhance vascular permeability in certain vessels in rat brain (30). BAY-u9773, an antagonist of both $CysLT_1R$ and $CysLT_2R$, functions at lower concentrations as a partial agonist of $CysLT_2R$ (31). In our study, BAY-u9773 superfusion of the tissue may elicit an initial stimulation of $CysLT_2R$ (transcellular vesicle transport mechanism initiation), followed by antagonist activity (FITC-albumin accumulation; **Fig. 8**). In line with this reasoning, after inhibition of $CysLT_2R$ with BAY-u9773 followed by subsequent stimulation with CysLTs, a very strong, immediate abluminal release of FITC-albumin into the extravascular compartment is observed. Interestingly, the absence of FITC-albumin accumulation in the vessel wall of MBCD-pretreated vessels after CysLT stimulation (Fig. 7*C*) further supports that blockade of caveolae, and subsequent vesicle formation attenuates CysLT-induced transcytosis and perhaps initiates a compensatory switch to paracellular transport, as has been described previously for caveolin-1 null mice (23). This point will have to be verified in future experiments.

Calcium signaling in acute vascular hyperpermeability responses (*e.g.*, histamine) is well-recognized *via* Ca^{2+}-calmodulin initiation of a cascade leading to contraction of endothelial cells and opening of intercellular junctions (14). Prolonged signaling (*e.g.*, thrombin) generates similar cellular events, as well as protein tyrosine phosphorylation and RhoA activation (32). Ca^{2+} signaling in transcellular vesicle transport-mediated vascular hyperpermeability has been postulated but never rigorously proven (14). Nevertheless, some clues have been collected. For example, vascular endothelial growth factor (VEGF) has been shown to stimulate enhanced vascular permeability *via* transcellular vesicles, and Ca^{2+} signals seem to be involved in forming, joining, and releasing the vesicles (33). Recent studies have demonstrated that CysLT stimulation of human umbilical vein endothelial cells predominantly expressing the $CysLT_2R$, as opposed to $CysLT_1R$, causes a potent Ca^{2+} spike followed by an oscillating Ca^{2+} signal (21). Taking into account the increased number of FITC-albumin accumulating sites after CysLT + BAY-u9773 treatment, thapsigargin addition, or CysLT stimulation in BAPTA-pretreated vessels, we speculate that an initial Ca^{2+} signal evoked by CysLT stimulation of $CysLT_2R$ leads to vesicle formation and endocytosis at luminal sites of endothelial cells (Fig. 8) similar to the VEGF model described by Bates (33). The $CysLT_2R$-triggered oscillating Ca^{2+} signal described

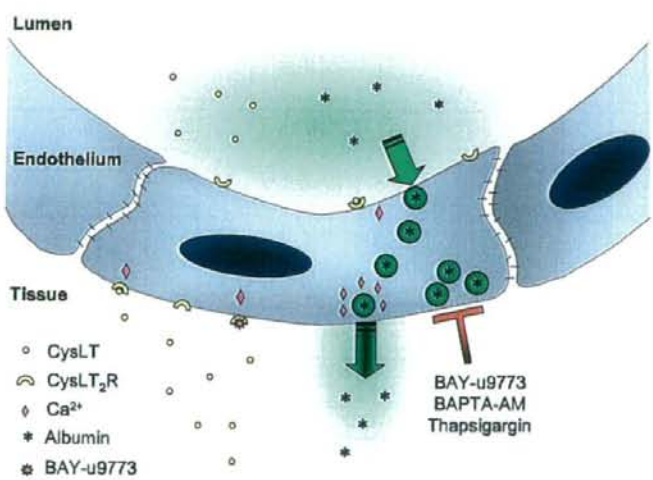

Figure 8. Model of $CysLT_2R$-regulated vascular leakage. Activation of $CysLT_2R$ by CysLTs or by the partial agonist activity of BAY-u9773 (31) results in a Ca^{2+} signal in the endothelial cell, which can also be mimicked by thapsigargin treatment. This Ca^{2+} signal stimulates vesicle formation and endocytosis at the luminal side, allowing the cell to accumulate albumin. The albumin-filled vesicles are transported to the abluminal side. Exocytosis of the albumin-filled vesicles and resultant vascular hyperpermeability is likely triggered by an oscillating Ca^{2+} signal (21) that is induced by CysLT-stimulation of the $CysLT_2R$. This oscillating Ca^{2+} signal can be blocked by the $CysLT_2R$ antagonist activity of BAY-u9773, by intracellular chelation with BAPTA, or by emptying intracellular stores with thapsigargin. This prevents exocytosis and causes an accumulation of albumin-filled vesicles inside the endothelial cell.

previously (21), on the other hand, could be the key to exocytosis at the abluminal side. The importance of Ca^{2+} signaling for exocytosis has been studied in detail for nerve cells (34) and has also been shown in astrocytes (35) and adrenal chromaffin cells (36). There has been speculation that it might be a more general mechanism also found in endothelial cells (14, 37), and our results contribute to and support this hypothesis.

In summary, our studies provide evidence for CysLT-mediated vascular permeability alterations exclusively *via* $CysLT_2R$ by means of transcellular endothelial vesicle transport, which is likely mediated by oscillatory Ca^{2+} signaling. Understanding and controlling this vascular hyperpermeability response is likely to be of importance for managing the clinical response to vascular injury and perhaps for preventing post-traumatic injury edema formation. However, since there are some differences in $CysLT_2R$ expression patterns between mice and humans (13, 38, 39), caution will have to be exercised before translating this work to human vascular disorders. FJ

We thank Dr. Yves St. Pierre (University of Quebec) for kindly supplying the murine b-end.3 cells. This work was supported by Canadian Institutes of Health Research grant MOP-68930 and the Canadian Foundation for Innovation. C.D.F. holds a Tier I Canada Research Chair in Molecular, Cellular, and Physiological Medicine and is recipient of a Career Investigator Award from the Heart and Stroke Foundation of Ontario. M.P.W.M. was supported by the German Academy of Sciences Leopoldina with the German Federal Ministry of Education and Research, BMBF-LPD 9901/8-132.

REFERENCES

1. Aller, M. A., Arias, J. L., Sánchez-Patán, F., and Arias, J. (2006) The inflammatory response: an efficient way of life. *Med. Sci. Monit.* **12,** RA225–234
2. Choilcain, N. N., and Redmond, H. P. (2006) Cell response to surgery. *Arch. Surg.* **141,** 1132–1140
3. Shiels, I. A., Taylor, S. M., and Fairlie, D. P. (2000) Cell phenotype as a target of drug therapy in chronic inflammatory diseases. *Med. Hypotheses* **54,** 193–197
4. Funk, C. D. (2001) Prostaglandins and leukotrienes: advances in eicosanoid biology. *Science* **294,** 1871–1875
5. Ciana, P., Fumagalli, M., Trincavelli, M. L., Verderio, C., Rosa, P., Lecca, D., Ferrario, S., Parravicini, C., Capra, V., Gelosa, P., Guerrini, U., Belcredito, S., Cimino, M., Sironi, L., Tremoli, E., Rovati, G. E., Martini, C., and Abbracchio, M. P. (2006) The orphan receptor GPR17 identified as a new dual uracil nucleotides/cysteinyl-leukotrienes receptor. *EMBO J.* **25,** 4615–4627
6. Funk, C. D. (2005) Leukotriene modifiers as potential therapeutics for cardiovascular disease. *Nat. Rev. Drug Discov.* **4,** 664–672
7. Lötzer, K., Funk, C. D., and Habenicht, A. J. (2005) The 5-lipoxygenase pathway in arterial wall biology and atherosclerosis. *Biochim. Biophys. Acta* **1736,** 30–37
8. Helgadottir, A., Manolescu, A., Thorleifsson, G., Gretarsdottir, S., Jonsdottir, H., Thorsteinsdottir, U., Samani, N. J., Gudmundsson, G., Grant, S. F., Thorgeirsson, G., Sveinbjornsdottir, S., Valdimarsson, E. M., Matthiasson, S. E., Johannsson, H., Gudmundsdottir, O., Gurney, M. E., Sainz, J., Thorhallsdottir, M., Andresdottir, M., Frigge, M. L., Topol, E. J., Kong, A., Gudnason, V., Hakonarson, H., Gulcher, J. R., and Stefansson, K. (2004) The gene encoding 5-lipoxygenase activating protein confers risk of myocardial infarction and stroke. *Nat. Genet.* **36,** 233–239
9. Dwyer, J. H., Allayee, H., Dwyer, K. M., Fan, J., Wu, H., Mar, R., Lusis, A. J., and Mehrabian, M. (2004) Arachidonate 5-lipoxygenase promoter genotype, dietary arachidonic acid, and atherosclerosis. *N. Engl. J. Med.* **350,** 29–37
10. Hui, Y., Cheng, Y., Smalera, I., Jian, W., Goldhahn, L., Fitzgerald, G. A., and Funk, C. D. (2004) Directed vascular expression of human cysteinyl leukotriene 2 receptor modulates endothelial permeability and systemic blood pressure. *Circulation* **110,** 3360–3366
11. Jiang, W., Hall, S. R., Moos, M. P. W., Cao, R. Y., Ishii, S., Ogunyankin, K. O., Melo, L. G., and Funk, C. D. (2008) Endothelial cysteinyl leukotriene 2 receptor ($CysLT_2R$) expression mediates myocardial ischemia-reperfusion injury. *Am. J. Pathol.* **172,** 592–602
12. Beller, T. C., Maekawa, A., Friend, D. S., Austen, K. F., and Kanaoka, Y. (2004) Targeted gene disruption reveals the role of the cysteinyl leukotriene 2 receptor in increased vascular permeability and in bleomycin-induced pulmonary fibrosis in mice. *J. Biol. Chem.* **279,** 46129–46134
13. Hui, Y., Yang, G., Galczenski, H., Figueroa, D. J., Austin, C. P., Copeland, N. G., Gilbert, D. J., Jenkins, N. A., and Funk, C. D. (2001) The murine cysteinyl leukotriene 2 (CysLT2) receptor. cDNA and genomic cloning, alternative splicing, and *in vitro* characterization. *J. Biol. Chem.* **276,** 47489–47495
14. Mehta, D., and Malik, A. B. (2006) Signaling mechanisms regulating endothelial permeability. *Physiol. Rev.* **86,** 279–367
15. McCafferty, D. M., Craig, A. W., Senis, Y. A., and Greer, P. A. (2002) Absence of Fer protein-tyrosine kinase exacerbates leukocyte recruitment in response to endotoxin. *J. Immunol.* **168,** 4930–4935
16. Warren, M., Huizar, J. F., Shvedko, A. G., and Zaitsev, A. V. (2007). Spatiotemporal relationship between intracellular Ca2+ dynamics and wave fragmentation during ventricular fibrillation in isolated blood-perfused pig hearts. *Circ. Res.* **101,** e90–e101
17. Fleming, I., Fisslthaler, B., and Busse, R. (1995) Calcium signaling in endothelial cells involves activation of tyrosine kinases and leads to activation of mitogen-activated protein kinases. *Circ. Res.* **76,** 522–529
18. Gericke, M., Droogmans, G., and Nilius, B. (1993) Thapsigargin discharges intracellular calcium stores and induces transmembrane currents in human endothelial cells. *Pflügers Arch.* **422,** 552–557
19. El-Mestrah, M., and Kan, F. W. (1999) Ultrastructural and ultracytochemical features of secretory granules in the ampullary epithelium of the hamster oviduct. *Anat. Rec.* **255,** 227–239
20. Huang, Q., Xu, W., Ustinova, E., Wu, M., Childs, E., Hunter, F., and Yuan, S. (2003) Myosin light chain kinase-dependent microvascular hyperpermeability in thermal injury. *Shock* **20,** 363–368
21. Lötzer, K., Spanbroek, R., Hildner, M., Urbach, A., Heller, R., Bretschneider, E., Galczenski, H., Evans, J. F., and Habenicht, A. J. (2003) Differential leukotriene receptor expression and calcium responses in endothelial cells and macrophages indicate 5-lipoxygenase-dependent circuits of inflammation and atherogenesis. *Arterioscler. Thromb. Vasc. Biol.* **23,** e32–36
22. Koopman, W. J., Scheenen, W. J., Schoolderman, L. F., Cruijsen, P. M., Roubos, E. W., and Jenks, B. G. (2001) Intracellular calcium buffering shapes calcium oscillations in Xenopus melanotropes. *Pflügers Arch.* **443,** 250–256
23. Predescu, D., Vogel, S. M., and Malik, A. B. (2004) Functional and morphological studies of protein transcytosis in continuous endothelia. *Am. J. Physiol. Lung Cell. Mol. Physiol.* **287,** L895–L901
24. Fredholm, B. B., Hökfelt, T., and Milligan, G. (2007) G-protein-coupled receptors: an update. *Acta Physiol.* **190,** 3–7
25. Casillan, A. J., Gonzalez, N. C., Johnson, J. S., Steiner, D. R., and Wood, J. G. (2003) Mesenteric microvascular inflammatory responses to systemic hypoxia are mediated by PAF and LTB4. *J. Appl. Physiol.* **94,** 2313–2322
26. Laemmel, E., Genet, M., Le Goualher, G., Perchant, A., Le Gargasson, J. F., and Vicaut, E. (2004) Fibered confocal fluorescence microscopy (Cell-viZio) facilitates extended imaging in the field of microcirculation. A comparison with intravital microscopy. *J. Vasc. Res.* **41,** 400–411
27. Ferri, L. E., Pascual, J., Seely, A. J., Chaudhury, P., and Christou, N. V. (2002) Soluble L-selectin attenuates tumor necrosis factor-alpha-mediated leukocyte adherence and vascular permeability:

a protective role for elevated soluble L-selectin in sepsis. *Crit. Care Med.* **30,** 1842–1847
28. Lominadze, D., Roberts, A. M., Tyagi, N., Moshal, K. S., and Tyagi, S. C. (2006) Homocysteine causes cerebrovascular leakage in mice. *Am. J. Physiol. Heart Circ. Physiol.* **290,** H1206–1213
29. Ghitescu, L., Fixman, A., Simionescu, M., and Simionescu, N. (1986) Specific binding sites for albumin restricted to plasmalemmal vesicles of continuous capillary endothelium: receptor-mediated transcytosis. *J. Cell Biol.* **102,** 1304–11
30. Hashizume, K., and Black, K. L. (2002) Increased endothelial vesicular transport correlates with increased blood-tumor barrier permeability induced by bradykinin and leukotriene C4. *J. Neuropathol. Exp. Neurol.* **61,** 725–735
31. Nothacker, H. P., Wang, Z., Zhu, Y., Reinscheid, R. K., Lin, S. H., and Civelli, O. (2000) Molecular cloning and characterization of a second human cysteinyl leukotriene receptor: discovery of a subtype selective agonist. *Mol. Pharmacol.* **58,** 1601–1608
32. Van Nieuw Amerongen, G. P., Draijer, R., Vermeer, M. A., and van Hinsbergh, V. W. (1998) Transient and prolonged increase in endothelial permeability induced by histamine and thrombin: role of protein kinases, calcium, and RhoA. *Circ. Res.* **83,** 1115–1123
33. Bates, D. O., Hillman, N. J., Williams, B., Neal, C. R., and Pocock, T. M. (2002) Regulation of microvascular permeability by vascular endothelial growth factors. *J. Anat.* **200,** 581–597
34. Rusakov, D. A. (2006) Ca2+-dependent mechanisms of presynaptic control at central synapses. *Neuroscientist* **12,** 317–326
35. Chen, X. K., Xiong, Y. F., and Zhou, Z. (2006) "Kiss-and-run" exocytosis in astrocytes. *Neuroscientist* **12,** 375–378
36. García, A. G., García-De-Diego, A. M., Gandía, L., Borges, R., and García-Sancho, J. (2006) Calcium signaling and exocytosis in adrenal chromaffin cells. *Physiol. Rev.* **86,** 1093–1131
37. Oheim, M., Kirchhoff, F., and Stühmer, W. (2006) Calcium microdomains in regulated exocytosis. *Cell Calcium* **40,** 423–439
38. Heise, C. E., O'Dowd, B. F., Figueroa, D. J., Sawyer, N., Nguyen, T., Im, D. S., Stocco, R., Bellefeuille, J. N., Abramovitz, M., Cheng, R., Williams, D. L. Jr., Zeng, Z., Liu, Q., Ma, L., Clements, M. K., Coulombe, N., Liu, Y., Austin, C. P., George, S. R., O'Neill, G.P., Metters, K. M., Lynch, K. R., and Evans, J. F. (2000) Characterization of the human cysteinyl leukotriene 2 receptor. *J. Biol. Chem.* **275,** 30531–30536
39. Ogasawara, H., Ishii, S., Yokomizo, T., Kakinuma, T., Komine, M., Tamaki, K., Shimizu, T., and Izumi, T. (2002) Characterization of mouse cysteinyl leukotriene receptors mCysLT1 and mCysLT2: differential pharmacological properties and tissue distribution. *J. Biol. Chem.* **277,** 18763–18768

Received for publication May 9, 2008.
Accepted for publication August 14, 2008.

厚生労働科学研究費補助金

長寿科学総合研究事業

高齢者呼吸器疾患の発症・制御に関与する遺伝子
・蛋白系の解明と治療応用に関する研究

平成20年度　総括・分担研究報告書

発行　平成21年3月31日

発行者「高齢者呼吸器疾患の発症・制御に関与する遺伝子
・蛋白系の解明と治療応用」

研究代表者　長瀬　隆英
〒113-8655
東京都文京区本郷 7-3-1
東京大学医学部附属病院